

Electrochemical characterization of microelectrodes for use in cortical tissue

Katie L. Harrigan^a, Ariba Chowdhury^b, Devang Gandhi^c, Ronnie Das^c, Patrick Rousche^c
 a Department of Applied Biology and Biomedical Engineering, Rose-Hulman Institute of Technology, Terre Haute, IN
 b Department of Biomedical and Chemical Engineering, Syracuse University, Syracuse, NY
 c Neural Engineering Device and Development Laboratory, University of Illinois at Chicago, Chicago, IL

Brain activity produces electrical activity which can be detected from within the cortical tissue of the brain. Brain Machine Interfaces (BMI's) have the potential to record and send these electrical signals through electrodes to facilitate communication between computer systems and the human brain.



Fig. 1. Basic design of a generic BMI system. Signals from the brain are acquired from electrodes and are then processed through a series of steps to extract specific features which reflect the motor intent. These signals are then translated into a signal that is read by and command device (Schalk et al. 2004).

Advancement of BMI technology is contingent on the development of stable, high performance electrodes which can be used in long-term implant systems. During insertion of the electrode, tissues and neurons are unavoidably damaged. However, it is believed that the damage zone could be minimized by using a smaller, more flexible electrode which could move freely within the dynamic environment of the brain, reducing the strain forces between the electrode surface and surrounding tissues which [4].

Cyclic voltammetry (CV) traces the transfer of electrons during oxidation-reduction reactions that occur as the electrode potential changes. Electronic impedance spectroscopy (EIS) utilizes a sinusoidal current signal applied to the electrochemical cell and then measures the elicited current from the electrode of interest to determine the impedance of the system.

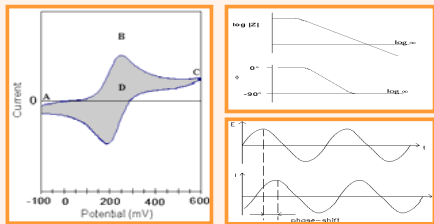


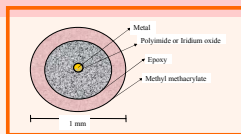
Fig. 2. (a) A cyclic voltammogram of a typical but non-specific metal. The total charge transfer of an electrode is defined by the area under the curve (D). (b) The typical output format for EIS as a bode plot where both magnitude (Z) and phase (Φ) of the impedance is reported. Pseudo-linearity of the system is illustrated by the resulting sinusoid shift only in phase and magnitude, but equal in frequency. Figure (b) was modified from <http://www.gamry.com>.

Materials and methods

A. Electrode Fabrication

- Metal Wires
 - Stainless Steel (diameter = 125 μm)
 - Gold (diameter = 76.2 μm)
- Coatings
 - Stainless Steel = 0.5 μm of Polyimide (prefabricated)
 - Gold = 0.5 μm Iridium Oxide (Electrodeposited)
- Stability and Sealant
 - ≈ 1 mm of methyl methacrylate and epoxy

Fig. 3. Cross sectional diagram of the electrode viewed perpendicular to the electrode surface. The diameter of the coated or uncoated metal wire is exaggerated in this representation for better illustration.



B. Electrodeposition of Iridium Oxide

- Aqueous Solution of an equilibrium solution of $\text{Ir}^{3+}/\text{Ir}^{4+}$ as prepared by Yamamaka [8] and Marzouk et al. [9]
 - HCl and KOH were used to adjust the solution's pH to 10.4
- Deposition
 - Triangular Waveform
 - o Cycled 50 time at 50 mV/s from 0V - 0.55 V
 - Rectangular Potential Pulses
 - o 1600 0.5 s pulses (0V, 0.55 V)

C. Electrochemical Measurements

- Electrochemical Cell Setup
 - Counter electrode = Platinum rod (surface area = 30 mm^2)
 - Reference electrode = Ag/AgCl
 - Electrolytes
- Cyclic Voltammetry
 - Working electrode cycled within the water window limits (-0.6 to 0.8 V)
- Electronic Impedance Spectroscopy (EIS)
 - Galvanostatic sinusoidal waveform ($A = 1 \mu\text{A}$ rms, $f = 0.01$ -100kHz)
- Data was analyzed using software custom-written in Matlab

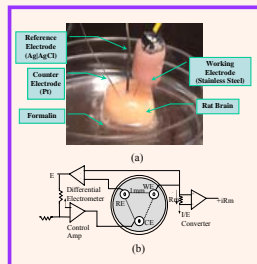


Fig. 4. (a) Schematic of the electrochemical cell. For testing, three different electrolytes are examined: phosphate buffer solution (PBS pH 7.4 ± 0.1), 10% formaldehyde fixing solution (formalin) and formalin fixed rat brain tissue. During fluid testing, the microelectrode array lies in a 100 mL beaker which is filled with 75 mL of solution. (b) Tissue testing follows the same setup but the beaker is replaced by a 100 mm culture dish which the tissue rests upon.

Results

A. Stainless Steel

CV of the stainless steel electrode revealed that each voltage scan resulted in a lower peak value of current and TACT than the previous curve (TCCT remained relatively stable). However, after the electrode is used in EIS testing, the peak value of current, TACT and TCCT resulting from the CV is much larger. The cause of this phenomena was determined to be the chromium oxide layer which forms on stainless steel depleting causing the properties to change, so for testing, special considerations needed to be made.

The stainless steel electrode had the largest overall charge transfer in saline with 30667.96 $\mu\text{C}/\text{cm}^2$. In formalin and brain tissue the overall charge transfer was 17199.64 and 17628.81 $\mu\text{C}/\text{cm}^2$ respectively. In saline, the impedance magnitude at higher frequencies (10 Hz - 100 kHz) was larger, but as the frequency decreased, the magnitude decreased. This is an expected result in reference to an equivalent circuit with mixed kinetic and charge transfer control as shown in Fig. 5.

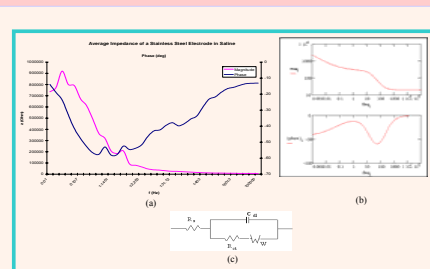


Fig. 5. (a) EIS bode plot of a stainless steel electrode in saline when cycled from 0.01 Hz - 100000 Hz. (b) EIS bode plot of the equivalent circuit (c) using Warburg coefficient ($W_w = 150 \text{ W sec}^{-1/2}$, $R_s = 200 \Omega$, $R_{ct} = 250 \Omega$, and $C_{dl} = 40 \mu\text{F}$). For diffusion processes, which adds a new form of resistance, a new element is added to the circuit and is referred to as the Warburg impedance. Areas of similarity to the stainless steel electrode can be found in the 0.01 Hz - 100000 Hz range.

B. Gold

It was determined from testing that gold is not readily oxidized in air, so no reoxidation period was necessary and each test was run in succession.

Once again, saline resulted in the largest overall charge transfer with 4438.37 $\mu\text{C}/\text{cm}^2$ and formalin and brain tissue were similarly less with 825.21 and 715.46 $\mu\text{C}/\text{cm}^2$ respectively. When compared to the stainless steel electrode, the magnitude of impedance for the gold electrode is significantly larger which could be the cause of the reduction in charge transfer capabilities. It was found that the gold system still follows the same mixed control circuit model which was used to describe the stainless steel electrode.

C. Iridium Oxide

As expected, the iridium oxide coating applied to the gold electrode greatly increased its charge transfer capabilities. After coating, the total charge transfer of the electrode in saline, formalin and brain tissue increased to 467809.12, 108593.53 and 60784.31 $\mu\text{C}/\text{cm}^2$ respectively. It was noticed however, that with time the iridium oxide coat was reducing. Knowing this, it is possible that the charge transfer in both formalin and brain tissue, which was tested after saline testing, would be higher if tested with a fresh iridium coating. The impedance for the iridium oxide resulted in more complex behavior than the stainless steel or pure gold due to the degradation of the coating. As the coating degraded, it became porous and the entering caused a new liquid-metal interface that added a factor to the electrode model.

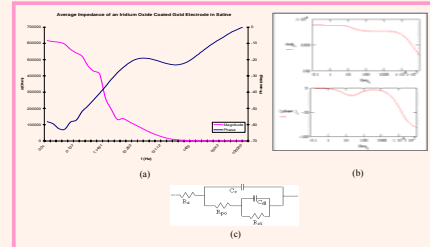


Fig. 6. (a) EIS bode plot of an iridium oxide coated gold electrode in saline when cycled from 0.01 Hz - 100000 Hz. (b) EIS bode plot of the equivalent circuit (c) using $C = 4 \text{ nF}$ calculated for a 10 cm^2 area, $\epsilon_r = 6$ and 12 μF thickness, $R_{po} = 3400 \Omega$ (assumed), $C_{dl} = 4 \text{ nF}$ calculated for 1% of 10 cm^2 area and assuming 40 $\mu\text{F}/\text{cm}^2$, $R_{ct} = 2500 \Omega$ assuming $k = 0.01 \text{ S}/\text{cm}$, $R_k = 20 \Omega$ calculated for 1% of 10 cm^2 area. For this model, the capacitance of the intact coating is represented by C. Pure resistance (R_{po}) is the resistance of ion conducting paths that develop in the coating.

TABLE I
COMPARISON OF DIFFERENT CHROMIUM OXIDE FILMS POLYIMIDE-BASED STAINLESS STEEL, GOLD AND IRIDIUM OXIDE COATED GOLD ELECTRODES BASED ON ELECTROCHEMICAL MEASUREMENTS

Electrode Type	Area	Scan Rate	Scan Range	Scan Type	Peak Current	Peak Potential	Peak Width	Peak Area	Peak Width	Peak Area
Stainless Steel	125 μm	50 mV/s	0V - 0.55V	Triangular	1.50E-05	0.15V	0.05V	1.50E-05	0.15V	0.05V
Gold	76.2 μm	50 mV/s	0V - 0.55V	Triangular	1.50E-05	0.15V	0.05V	1.50E-05	0.15V	0.05V
Iridium Oxide	76.2 μm	50 mV/s	0V - 0.55V	Triangular	1.50E-05	0.15V	0.05V	1.50E-05	0.15V	0.05V

TABLE II
COMPARISON OF DIFFERENT CHROMIUM OXIDE FILMS POLYIMIDE-BASED STAINLESS STEEL, GOLD AND IRIDIUM OXIDE COATED GOLD ELECTRODES BASED ON ELECTROCHEMICAL MEASUREMENTS

Electrode Type	Area	Scan Rate	Scan Range	Scan Type	Peak Current	Peak Potential	Peak Width	Peak Area	Peak Width	Peak Area
Stainless Steel	125 μm	50 mV/s	0V - 0.55V	Triangular	1.50E-05	0.15V	0.05V	1.50E-05	0.15V	0.05V
Gold	76.2 μm	50 mV/s	0V - 0.55V	Triangular	1.50E-05	0.15V	0.05V	1.50E-05	0.15V	0.05V
Iridium Oxide	76.2 μm	50 mV/s	0V - 0.55V	Triangular	1.50E-05	0.15V	0.05V	1.50E-05	0.15V	0.05V

Conclusions

Based on testing, gold coated with iridium oxide would be most effective as a neural stimulation electrode if there were a method of application which would ensure long term stability of the coating. The iridium oxide coating offers low impedance and high charge transfer capabilities to a gold electrode. It is known from previous work that when appropriately applied, iridium oxide is biocompatible [11] and using gold as a base ensures that should the coating be lost, metal will not be readily lost to the biological environment as would be the case of stainless steel electrodes. In the future, more work needs to be done on methods of coating electrodes as well as better models of the electrode need to be made for effective comparison. It is also proposed to add a new component to the system models in order to emulate the oscillations that would be seen when an electrode is implanted into a living being. It is possible this resistance would be so high as to limit the effectiveness of the electrode as a stimulator or recorder.

Literature cited

- [1] Schalk, Andrew. "Journal of Neural Engineering." Ann. Rev. Neurosci. 27 (2004): 487-507.
- [2] Webster, J.G. Medical Instrumentation: Application and Design, Third Edition. Canada: John Wiley & Sons, Inc., 1998.
- [3] Maynard E.M., Fernandez E., and Norman R.A. "A technique to prevent dural adhesion to chronically implanted microelectrode arrays." *Journal of Neuroscience Methods*, 97(2000): 93-101.
- [4] Rousche P. J., Pellmar, D. S., Pivov D. P., Williams J. C., Vetter R. J., and Kiper D. R., "Flexible Polyimide-Based Intracortical Electrodes: Array with Resective Capabilities." *IEEE Trans. Biomed. Eng.*, vol. 48, pp.184-173, Mar. 2002.
- [5] J.D. Weiland, D.J. Anderson, M. S. Hamoun, "In Vivo Electrical Properties for Iridium Oxide Versus Titanium Nitride Stimulating Electrodes." *IEEE Trans. Biomed. Eng.*, vol. 49, pp.1574-1579, Dec. 2002.
- [6] McCreey D.H., Agnew Y.G., Voss T.G. III, and Billara L., "Charge Density and Charge Per Pulse as Co-factors in Neural Injury Induced by Electrical Stimulation." *IEEE Transactions on Biomed. Eng.*, vol. 37, pp.966-980, Oct. 1990.
- [7] Roubicek, S., Lefkovic, L., and Brummer S. B., "Activated Ir: An electrode suitable for reversible charge injection in saline." *J. Electrochem. Soc.*, vol. 130, pp. 1683-1687, 1983.
- [8] Yamamaka K., "Anodically Electrodeposited Iridium Oxide Films (AEIROF) from Aqueous Solutions for Electrochemical Display Devices." *Jpn. J. Appl. Phys.*, vol. 28, pp.452-457, 1989.
- [9] Marzouk S. A. M., Uter A., Basak R. P., Johnson Dandekar, A., and Cascio W. E., "Electrodeposited Iridium Oxide pH electrode for Measurement of Extracellular Myocardial Acidosis During Acute Ischemia." *Anal. Chem.*, vol. 70, pp.5054-5061, 1998.
- [10] *Electrochemical Impedance: Analysis and Interpretation*, J.R. Scully, D.C. Silverman, and M.W. Kang, editors, ASTM, 1993.

Acknowledgments

The author would like to thank the members of the Neural Engineering Device and Development Laboratory and the Neural Engineering Applications Laboratory at the University of Illinois at Chicago for all the support and guidance given for this research project. Thanks to the National Science Foundation and the Research Experience for Undergraduates Program at University of Illinois at Chicago for support and funding of this work.